



Peer review status:

This is a non-peer-reviewed preprint submitted to EarthArXiv.

GEDIMetrics: a QGIS plugin for accessing and integrating multi-product GEDI spaceborne LiDAR data

Alexander Cotrina-Sanchez ^{a,b,*}, Michele Torresani ^a, and Leonel Corado ^c

^a Free University of Bozen/Bolzano, Faculty of Agricultural, Environmental and Food Sciences, Piazza Università/Universitätsplatz, 39100, Bozen/Bolzano, Italy

^b Instituto de Investigación para el Desarrollo Sustentable de Ceja de Selva (INDES-CES), Universidad Nacional Toribio Rodríguez de Mendoza de Amazonas, Chachapoyas 01001, Peru

^c MED – Mediterranean Institute for Agriculture, Environment, and Development, CHANGE – Global Change and Sustainability Institute, Institute for Advanced Studies and Research, Universidade de Évora, Pólo da Mitra, Ap. 94, 7006-554, Évora, Portugal

*Correspondence author: danyalexander.cotrinasanchez@unibz.it

Abstract

NASA's Global Ecosystem Dynamics Investigation (GEDI) provides near-global, high-resolution 3D LiDAR observations of forest vertical structure. However, GEDI products are distributed as independent HDF5 files organised by beam, requiring ad-hoc workflows for data discovery, quality filtering, spatial subsetting, and footprint-level alignment across products. Existing tools either target a single product, require programming expertise, or operate outside common GIS environments. Here, GEDIMetrics is presented as an open-source QGIS plugin that integrates the full GEDI processing chain for four products focused on forest vertical structure: canopy height (L2A), vertical canopy structure (L2B), aboveground biomass density (L4A), and waveform structural complexity (L4C). The plugin implements a five-stage pipeline: granule discovery via the NASA CMR API, authenticated download, variable extraction with quality filtering, spatial subsetting, and multi-product merging using the shot_number identifier, with export to GeoPackage and GeoParquet. Its core contribution is the automated footprint-level fusion of these products into a single analysis-ready dataset through a graphical interface, without scripting. GEDIMetrics was tested across two contrasting forest ecosystems (~100 km² each): a temperate mixed forest in northeastern France and a humid tropical rainforest in Madre de Dios, Peru. The plugin is freely available through the QGIS Plugin Repository and on GitHub.

Keywords: Earth observation, GEDI, GIS, forest structure, remote sensing, waveform lidar

1. Introduction

Forests are key carbon reservoirs and critical regulators of the global climate system (FAO 2025), while their three-dimensional structure underpins carbon storage and dynamics, biodiversity, habitat quality, and sustainable forest management across scales (Goetz and Dubayah 2011). Conventional approaches, such as ground-based inventories and airborne laser scanning (ALS), provide high-accuracy measurements but are logistically constrained, costly at large scales, and spatially discontinuous, often requiring multisource data integration (Næsset et al. 2011; Coops et al. 2023; Meng et al. 2026). Satellite remote sensing provides consistent, large-scale observations; however, optical and radar data are limited in their ability to directly resolve vertical forest structure and typically require LiDAR data for structural characterization (Pardini et al. 2019). Spaceborne missions (e.g., ICESat-2) have extended LiDAR observations to high-

39 latitude and boreal regions (Markus et al. 2017), while NASA's Global Ecosystem Dynamics
40 Investigation (GEDI) represents a major advance in the detailed characterization of forest vertical
41 structure at near-global scale (Dubayah et al. 2020a).

42 Mounted aboard the International Space Station (ISS) since 2018, GEDI provides near-global sampling of
43 forest structure between 51.6°N and 51.6°S through billions of laser waveforms, known as footprints,
44 delivering detailed information on vegetation vertical structure across multiple data products (Dubayah et
45 al. 2020a; Hakkenberg et al. 2023). Level 2A product provides canopy height and ground elevation
46 metrics (Dubayah et al. 2020b), Level 2B characterises vertical canopy structure (e.g., canopy cover, plant
47 area index, foliage profiles) (Dubayah et al. 2021), and Level 4A delivers aboveground biomass density
48 (AGBD) estimates derived from globally calibrated models (Dubayah et al. 2022). The Level 4C product
49 provides footprint-level estimates of the Waveform Structural Complexity Index (WSCCI), a metric
50 describing three-dimensional canopy structural complexity derived from machine-learning models trained
51 on collocated GEDI and airborne LiDAR data (De Conto et al. 2024). Together, these products support a
52 wide range of ecological and environmental applications, including forest carbon mapping, biodiversity
53 assessment, natural disturbance monitoring, and the calibration and validation of satellite-based
54 vegetation models (Vogeler et al. 2023; De Conto et al. 2024; Torresani et al. 2026). However, integrating
55 these complementary datasets remains technically challenging, as they are distributed as independent
56 HDF5 files organised by each beam and require alignment via the *shot_number* identifier alongside
57 specialised workflows for data access, download, spatial subsetting, and filtering, posing a barrier for
58 many users in ecology, forestry, and geospatial analysis.

59 Several tools address individual components of the GEDI processing workflow but lack end-to-end
60 integration. NASA's EarthData Search portal supports data discovery and download but does not perform
61 subsetting, filtering, or cross-product integration (NASA 2026). Programmatic solutions such as rGEDI
62 (Silva et al. 2020), and pyGEDI (Serna and Hernandez-Serna 2020) enable flexible programmatic
63 processing but require coding expertise and do not provide unified workflows for multi-product analysis.
64 Unified workflow frameworks such as GEDI-Data-Resources (ref [https://github.com/nasa/GEDI-data-
65 resources](https://github.com/nasa/GEDI-data-resources)) and GEDI-Pipeline (Corado and Godinho 2025) introduce automation layers and simplified
66 execution pipelines, enabling stable and reproducible large-scale GEDI data retrieval through a single
67 command-line or Jupyter-based execution (Kluyver Thomas et al. 2016). However, these frameworks do
68 not provide a graphical user interface (GUI) suitable for non-programming users.

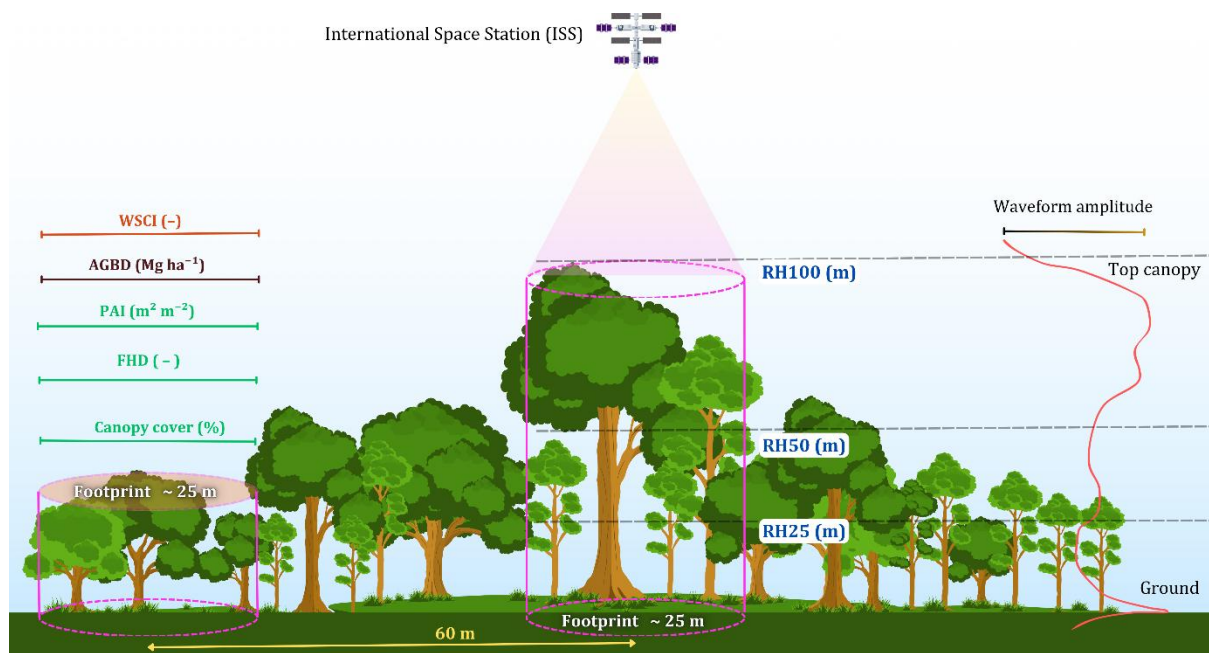
69 Other tools address specific tasks such as scalable database management or geolocation correction (Vangi
70 et al. 2023; Corado et al. 2025; Besnard et al. 2025), yet none are designed for interactive, GIS-based
71 analysis. Within the QGIS ecosystem, the most widely used open-source GIS platform globally (Graser et
72 al. 2025), numerous plugins exist for optical and SAR data processing (Congedo 2021; Martinoli et al.
73 2026). Recent developments such as the GEDI-Pipeline QGIS Plugin
74 (https://plugins.qgis.org/plugins/gedi_pipeline_plugin/) introduced graphical access to the GEDI data
75 workflow, lowering the technical barrier associated with command-line execution. However, the plugin
76 does not support integrated multi-product merging, advanced filtering operations or unified analysis of
77 GEDI structural and biomass products.

78 In this paper, GEDIMetrics is presented as an open-source plugin for QGIS (3.4 or higher) that addresses
79 this gap by integrating the full GEDI data processing chain into a single graphical workflow. The plugin
80 implements a modular pipeline comprising granule discovery, data download, spatial subsetting, quality
81 filtering, and multi-product merging based on the *shot_number* identifier, followed by export to standard
82 geospatial formats (e.g., GeoPackage, GeoParquet). Its core contribution lies in the automated fusion of
83 the L2A, L2B, L4A, and L4C GEDI data products into a single analysis-ready dataset for GIS-based

84 vegetation analysis. The structure of this paper is organised as follows: Section 2 presents the technical
 85 background of GEDI data products; Section 3 describes the architecture, processing pipeline, and user
 86 interface of GEDIMetrics; Section 4 describes the case study; Section 5 presents the results; Section 6
 87 discusses the methodological contribution, implications, and limitations; and Section 7 concludes.

88 2. GEDI spaceborne lidar data

89 GEDI data products are generated through a hierarchical processing chain from full-waveform LiDAR
 90 observations acquired from the ISS (Fig. 1). Each laser footprint (~25 m diameter) is spaced
 91 approximately 60 m along-track and captures the vertical distribution of returned energy, from which
 92 canopy height, vertical structure, biomass, and structural complexity metrics are derived at four
 93 processing levels (Table 1). All products are distributed as HDF5 files organised by beam group and
 94 require alignment via the *shot_number* identifier to enable cross-product integration. This data
 95 architecture, combined with the independent distribution of each product and the application of product-
 96 specific quality filters, introduces technical challenges for routine multi-product analysis. The joint use of
 97 L2A, L2B, L4A, and L4C enables integrated assessments of vegetation structure and biomass, supporting
 98 applications such as biomass modelling, disturbance detection, and validation of large-scale mapping
 99 products yet practical implementation remains constrained by the complexity of accessing, processing,
 100 and merging these datasets.



101

102 **Figure 1.** Figure 1. Conceptual representation of GEDI full-waveform LiDAR measurements and derived forest
 103 structural metrics. GEDI laser footprints (~25 m diameter), spaced ~60 m along-track, sample the vertical
 104 distribution of vegetation structure. L2A metrics (relative height, i.e., RH25, RH50, RH100), L2B metrics (plant
 105 area index, PAI; foliage height diversity, FHD; and canopy cover), L4A metrics (aboveground biomass density,
 106 AGBD), and L4C Waveform Structural Complexity Index (WSCl) are illustrated.

107

108

109

110 **Table 1.** Summary of GEDI data products supported by GEDIMetrics. For each product, the table lists the primary
 111 thematic domain, key variables available for extraction, associated quality flags used for filtering, and the original
 112 data reference.

Product	Domain	Key variables	Quality flags / filters	Reference
GEDI02_A (L2A)	Canopy height and ground elevation	RH0–RH100, elev_lowestmode, elev_highestreturn, selected_algorithm	quality_flag, degrade_flag, sensitivity	(Dubayah et al. 2020b)
GEDI02_B (L2B)	Vertical canopy structure	cover, PAI, FHD, PAI_z, PAVD_z (vertical profile)	l2b_quality_flag, degrade_flag, sensitivity, surface_flag	(Dubayah et al. 2021)
GEDI04_A (L4A)	Aboveground biomass density	AGBD, AGBD_se, AGBD_prediction, l4_quality_flag	l4_quality_flag, degrade_flag, sensitivity, selected_algorithm	(Dubayah et al. 2022)
GEDI04_C (L4C)	Structural complexity	WSCI, WSCI_se	l4c_quality_flag, degrade_flag, sensitivity	(De Conto et al. 2024)

113

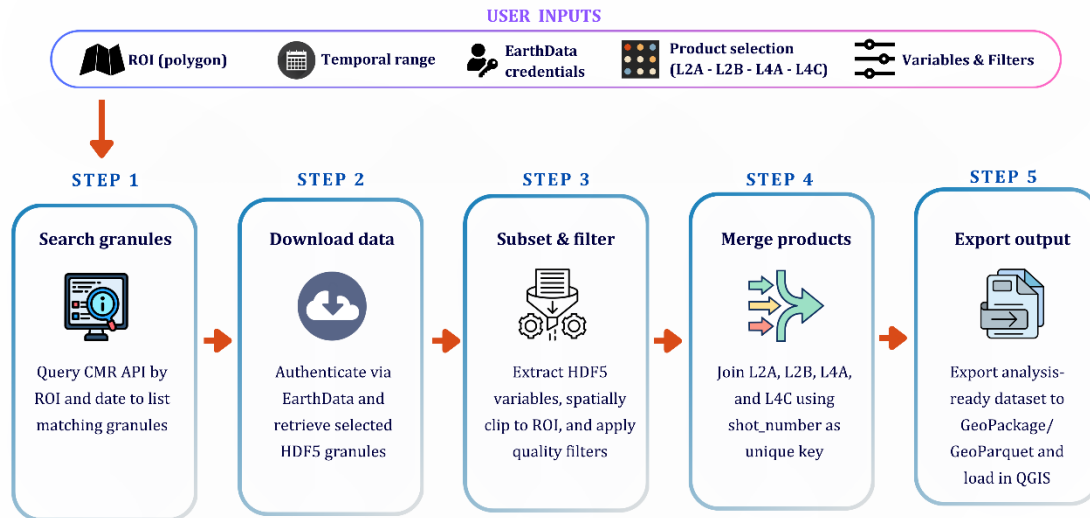
114 3. Design and implementation

115

116 3.1. Architecture and workflow

117 GEDIMetrics is implemented as a QGIS plugin in Python 3, compatible with QGIS versions 3.4 or
 118 higher. It follows a modular pipeline architecture comprising five sequential stages: orbit discovery, data
 119 download, subsetting, multi-product merging, and export. Each stage is encapsulated in an independent
 120 module and coordinated by a central pipeline controller, enabling flexible execution, error handling, and
 121 partial re-processing. Download operations are executed asynchronously to prevent the QGIS interface
 122 from becoming unresponsive during large data retrievals.

123 The workflow is configured through a graphical interface, where users specify target GEDI products
 124 (L2A, L2B, L4A, L4C), temporal range, region of interest (ROI), variables, quality filters, and output
 125 format. The system requires the NASA CMR (Common Metadata Repository) API (Application
 126 Programming Interface) to identify relevant granules and retrieves them via authenticated access to
 127 NASA EarthData. Each granule is then processed through variable extraction, quality filtering, and spatial
 128 clipping to the user-defined ROI. Product-specific outputs are integrated into a single dataset through a
 129 *shot_number* based join and exported to standard geospatial formats (Fig. 2).



130

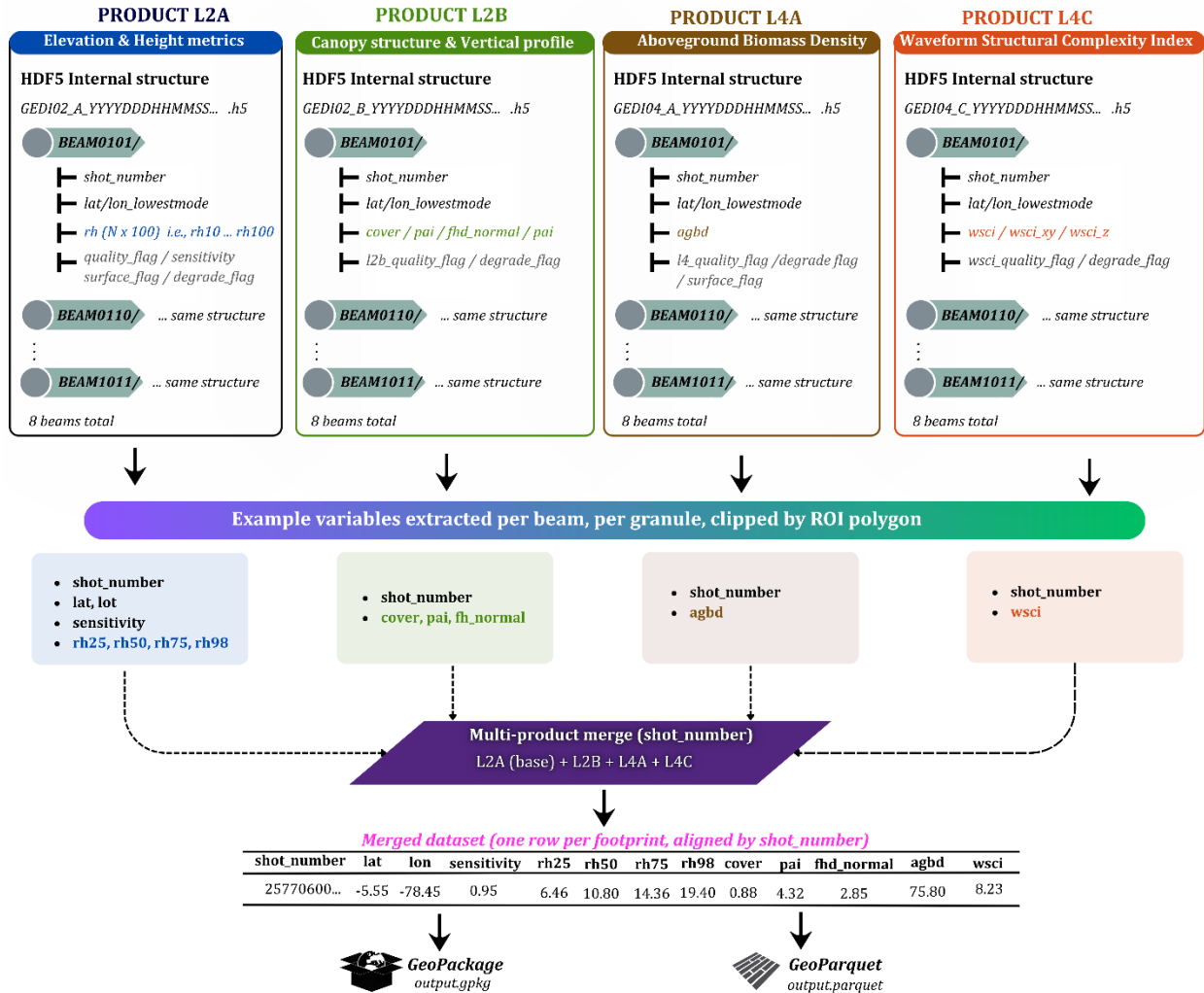
131 **Figure 2.** GEDIMetrics workflow illustrates the five-stage pipeline: granule discovery via CMR API, data download
 132 from EarthData, subsetting and quality filtering of HDF5 data, multi-product integration using shot_number, and
 133 export to GIS-compatible formats.

134 **3.2. Data Processing and Integration**

135 GEDI granules are stored in HDF5 format, with data organised by eight beam groups (four full-power and
 136 four coverage beams). The subsetting stage iterates over all beams within each granule, extracting user-
 137 selected variables together with essential metadata: coordinates, shot_number, acquisition time, and
 138 quality flags (Fig. 3). Spatial filtering is performed in two stages: an initial bounding-box pre-filter based
 139 on coordinate ranges for computational efficiency, followed by precise point-in-polygon clipping against
 140 the user-defined ROI using Shapely geometric operations. This two-stage approach substantially reduces
 141 processing time for large granules covering areas much wider than the target region.

142 The principal methodological contribution of GEDIMetrics is the automated, footprint-level integration of
 143 L2A, L2B, L4A, and L4C data using the shot_number identifier as a unique key (Fig. 3). Because each
 144 product undergoes independent processing and considering that data availability may differ across
 145 products due to variations in temporal coverage, algorithm convergence, or quality criteria, the number of
 146 retained footprints is generally not identical across products. To solve this, merging is performed
 147 sequentially using L2A as the base product, with configurable join strategies: an inner join retains only
 148 footprints present in all selected products, ensuring cross-product consistency, while an outer join
 149 preserves maximum spatial coverage at the cost of null values for missing fields. The resulting dataset
 150 contains one row per footprint, in which canopy height metrics (from L2A), vertical structure descriptors
 151 (from L2B), biomass estimates (from L4A), and structural complexity indices (from L4C) are aligned at
 152 the individual shot level (Fig. 3).

153 The merged dataset is exported in GeoPackage format for direct use within QGIS and other GIS
 154 environments, or in GeoParquet format for large-scale programmatic workflows in Python
 155 (<https://www.python.org/> or R (<https://cran.r-project.org/>) languages. Output files include embedded
 156 metadata recording the processing configuration: selected products, temporal range, ROI geometry,
 157 applied quality thresholds, merge strategy, plugin version, and processing timestamp, ensuring full
 158 reproducibility. GeoPackage merged output are automatically loaded into the active QGIS project.



159

160 **Figure 3.** Multi-product GEDI data processing and integration workflow. Variables are extracted per beam from
 161 L2A, L2B, L4A, and L4C HDF5 granules, spatially clipped to the user-defined region of interest, and merged at the
 162 footprint level using the shot_number identifier. The resulting dataset contains one row per footprint with variables
 163 from all selected products, exported in GeoPackage or GeoParquet format.

164 **3.3. User Interface and quality filtering**

165 The GEDIMetrics graphical interface provides an integrated environment for configuring all processing
 166 parameters without requiring programming expertise. The plugin is accessible through the QGIS Plugin
 167 Manager (Fig. 4a) and is organised into five tabbed panels.

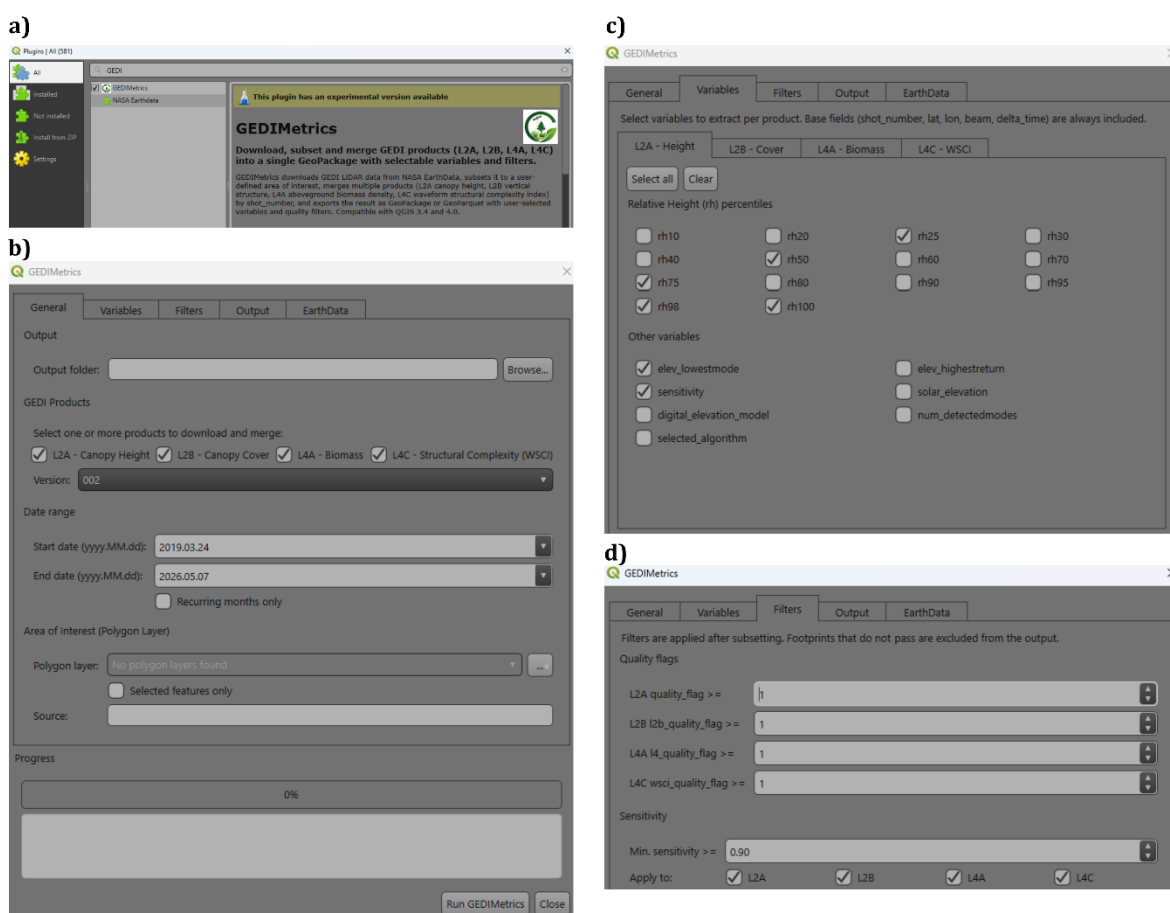
168 The General panel (Fig. 4b) allows users to select one or more GEDI products to download and merge
 169 (L2A – Canopy Height, L2B – Canopy Cover, L4A – Biomass, L4C – Structural Complexity), the product
 170 version, a temporal range with start and end dates, and the region of interest defined by a polygon layer
 171 loaded in the active QGIS project. An option to restrict processing to selected features within the polygon
 172 layer is provided, together with a recurring months filter for seasonal analyses.

173 The Variables panel (Fig. 4c) enables per-product variable selection through dedicated sub-tabs. For L2A,
 174 users can select individual relative height percentiles (RH10 to RH100) and auxiliary variables such as
 175 elev_lowestmode, elev_highestreturn, sensitivity, selected_algorithm, and solar_elevation. Equivalent

176 selection interfaces are provided for L2B (e.g., cover, PAI, FHD), L4A (e.g., AGBD, AGBD_se), and L4C
177 (e.g., WSCI, WSCI_xy, WSCI_z). A set of base fields: shot_number, latitude, longitude, beam, and
178 delta_time are always included in the output to ensure spatial referencing and traceability.

179 The Filters panel (Fig. 4d) controls quality constraints applied after subsetting. Product-specific quality
180 flags are configurable as minimum thresholds (default ≥ 1 for quality_flag, l2b_quality_flag,
181 l4_quality_flag, and wsci_quality_flag). A global minimum beam sensitivity threshold (default ≥ 0.90)
182 can be applied selectively to any combination of products through individual checkboxes, following the
183 criterion proposed by Potapov et al., (2021) for broad-scale applications; users may increase this value for
184 specific ecosystem types, such as ≥ 0.96 for temperate forests (Rajab Pourrahmati et al. 2023) or higher
185 for dense tropical canopies (Oliveira et al. 2023). Degraded footprints are excluded by default
186 (degrade_flag = 1), and surface type filtering allows restriction to land, water, or all surface types.

187 Additional tabs provide configuration for the output format (GeoPackage or GeoParquet) and EarthData
188 authentication credentials. Real-time feedback is provided through a progress indicator and logging panel
189 visible in the main interface, enabling transparent execution monitoring.



190
191 **Figure 4.** GEDIMetrics graphical user interface. (a) Plugin installation through the QGIS Plugin Manager. (b)
192 General panel for product selection (L2A, L2B, L4A, L4C), version, temporal range, and region of interest
193 configuration. (c) Variables panel showing per-product variable selection (L2A relative height percentiles and
194 auxiliary metrics illustrated); (d) Filters panel for quality flag thresholds, beam sensitivity, degradation exclusion,
195 and surface type filtering.

196 3.4. Software availability and requirements

197 GEDIMetrics is distributed as an open-source plugin through the official QGIS Plugin Repository (listed as
198 GEDIMetrics experimental version), enabling direct installation via the Plugin Manager or manually from the ZIP
199 archive available at <https://github.com/AlexanderCotrinas/gedi-metrics-qgis>. The current release (v1.0.2) is
200 compatible with QGIS 3.4 or higher and is released under the GNU General Public License v3.0 (GPL v3). A
201 permanently archived version is deposited at Zenodo (DOI: pending).

202 GEDIMetrics requires several Python libraries: h5py (HDF5 access), pandas and geopandas (tabular and spatial
203 data), shapely and fiona (geometry and file I/O), rtree (spatial indexing), and pyarrow (GeoParquet export). Libraries
204 pre-installed with QGIS (numpy, requests, PyQt5) require no additional action; the remaining dependencies are
205 automatically installed on first launch, or manually via pip if needed. On Windows, installation via the OSGeo4W
206 distribution is strongly recommended, as it provides pre-compiled geospatial binaries (GDAL, GEOS, PROJ) that
207 resolve common dependency conflicts; in that case, dependencies can be installed through the OSGeo4W Shell
208 using `pip install h5py geopandas pyarrow`. A valid NASA EarthData account (<https://urs.earthdata.nasa.gov>) is
209 required for data access.

210 4. Case study

211 4.1. Study areas

212 The performance of GEDIMetrics was evaluated across two contrasting forest ecosystems within the
213 GEDI sampling domain (Fig. 5): a temperate mixed forest in northeastern France, and a humid tropical
214 rainforest in the Peruvian Amazon, covering approximately 100 km² each study area. These sites were
215 selected to represent distinct structural, climatic, and ecological conditions, ensuring coverage of a broad
216 range of canopy complexity and biomass regimes, as well as differing GEDI acquisition characteristics.

217 The temperate study area (Fig. 5a) is located in northeastern France (~48.6°N, 6.6°E). According to the
218 Copernicus Land Monitoring Service Dominant Leaf Type (European Environment Agency 2024), the
219 forest composition is predominantly broadleaved, although smaller coniferous patches are also present
220 within and around the main forested area. Compared to the tropical site, GEDI observations at this
221 location benefit from improved ground return detection due to lower canopy density and deciduous
222 canopy gaps; however, the higher latitude results in lower footprint density, requiring broader temporal
223 windows for adequate data acquisition.

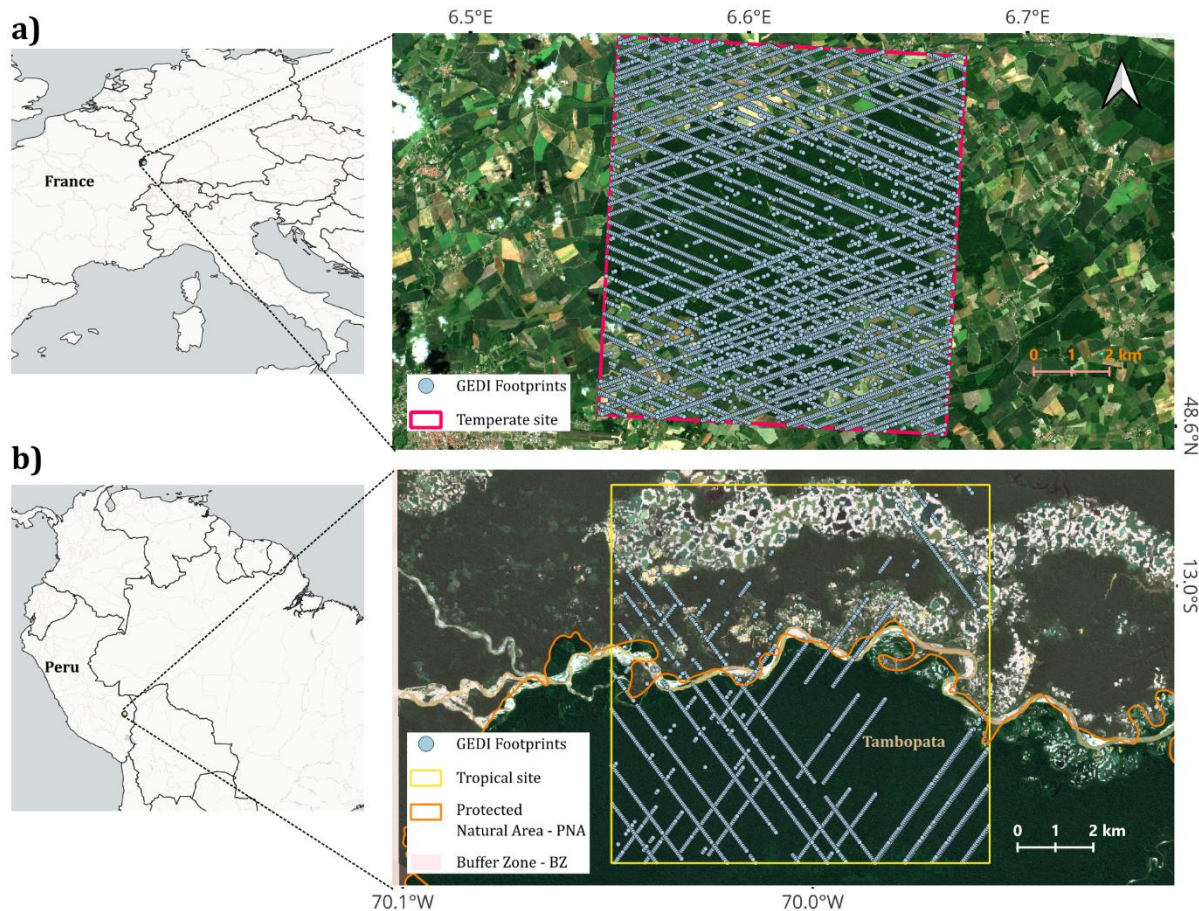
224 The tropical study area (Fig. 5b) is located in the Madre de Dios Department, southeastern Peru (~13.0°S,
225 70.0°W). The site partially overlaps the Tambopata National Reserve and its designated buffer zone, a
226 region where intact tropical forest is under increasing pressure from illegal gold mining and associated
227 deforestation (Caballero Espejo et al. 2018; Pacsi et al. 2026). This context makes the area particularly
228 relevant for monitoring forest structural degradation using active remote sensing tools. The site is
229 characterised by dense, multi-layered tropical canopies with high species diversity. From a GEDI
230 perspective, this environment presents challenging acquisition conditions: dense canopies attenuate the
231 laser signal, reducing ground return detection and increasing uncertainty in waveform-derived metrics.
232 These characteristics make the site well suited for evaluating quality filtering performance and footprint
233 retention under low-sensitivity conditions.

234 4.2. Processing configuration

235 For both study areas, GEDI data were acquired using GEDIMetrics with the following configuration:
236 products L2A, L2B, L4A, and L4C, version 002, temporal range from 2019-03-24 to 2023-04-01, and a
237 global minimum beam sensitivity threshold of 0.90 (Potapov et al. 2021). All other quality filters were

238 applied at default settings ($quality_flag \geq 1$, $degrade_flag$ excluded, $surface_flag = land$; Table 1, Fig. 4d).
239 Footprints were spatially clipped to each study area polygon and merged using an inner join to retain only
240 footprints with data across all selected products.

241 To focus the analysis on forested areas, a post-processing mask was applied using the annual forest/non-
242 forest classification from the Joint Research Centre (JRC) Global Forest Cover product (Bourgoin et al.
243 2024). Only footprints falling within pixels classified as forest were retained for subsequent analysis,
244 excluding non-forest land covers such as agricultural fields, water bodies, and cleared areas. This step
245 ensures that the integrated GEDI metrics correspond exclusively to forested conditions, enabling
246 meaningful comparison of structural and biomass variables across the two contrasting sites.



247
248 **Figure 5.** Location of the two study areas used to evaluate GEDIMetrics. (a) Temperate site in France
249 (~48.6°N, 6.6°E), covering approximately 100 km² of mixed temperate forest. (b) Tropical site in the
250 Madre de Dios Department, southeastern Peru (~13.0°S, 70.0°W), encompassing approximately 100 km²
251 partially overlapping the Tambopata National Reserve (PNA) and its buffer zone (BZ). Blue dots
252 represent GEDI footprints retrieved and processed by GEDIMetrics. Background imagery: Sentinel-2
253 scenes from July 2022.

254
255
256

257 5. Results

258 5.1. Data acquisition and footprint retention

259 GEDIMetrics was used to acquire and process GEDI data for both study areas using the full available
260 temporal range (March 2019 – March 2023), product v2, and default quality filtering parameters
261 (`quality_flag` ≥ 1 , `degrade_flag` excluded, `surface_flag` = land, `sensitivity` ≥ 0.90). Footprints lacking valid
262 coordinates were excluded, and a JRC forest/non-forest mask (Vancutsem et al., 2021) was applied to
263 restrict the analysis to forested areas. Table 3 summarises the acquisition outcomes and per-product
264 footprint availability for both sites.

265 Despite comparable ROI areas (~ 100 km²), the temperate site yielded substantially more granules and
266 forested footprints than the tropical site (96 vs. 23 granules; 5,939 vs. 1,712 footprints), reflecting the
267 higher GEDI revisit frequency at mid-latitudes due to ISS orbital geometry. Product-level availability
268 differed markedly between sites: L2B retention was moderate in the temperate site (60.8%) but nearly
269 absent in the tropical site (0.9%, $n = 16$), whereas L4A showed the inverse pattern (7.2% vs. 87.2%).
270 These asymmetries indicate that product-level data availability is strongly site-dependent and cannot be
271 assumed from L2A footprint counts alone.

272 Table 3. GEDI data acquisition and footprint retention for the temperate and tropical study areas. Quality
273 filtering was applied with default thresholds (`sensitivity` ≥ 0.90 , `quality_flag` ≥ 1 , `degrade_flag` excluded,
274 `surface_flag` = land). Product-level counts represent footprints with valid (non-null) values for each
275 product's key variable after forest masking; percentages are relative to the total forested footprints at each
276 site.

Parameter	Temperate (France)	Tropical (Peru)
Acquisition		
Granules identified	96	23
Raw data volume (GB)	~ 184	~ 80
Footprint filtering		
Total footprints (from plugin)	11,071	2,291
With valid coordinates	10,497	1,944
After JRC forest mask	5,939	1,712
Valid footprints per product		
L2A – Canopy Height	5,939 (100%)	1,712 (100%)
L2B – Canopy Cover	3,609 (60.8%)	16 (0.9%)
L4A – Biomass	430 (7.2%)	1,493 (87.2%)
L4C – Structural Complexity	4,940 (83.2%)	621 (36.3%)

277

278 5.2. Forest structure and biomass characterization

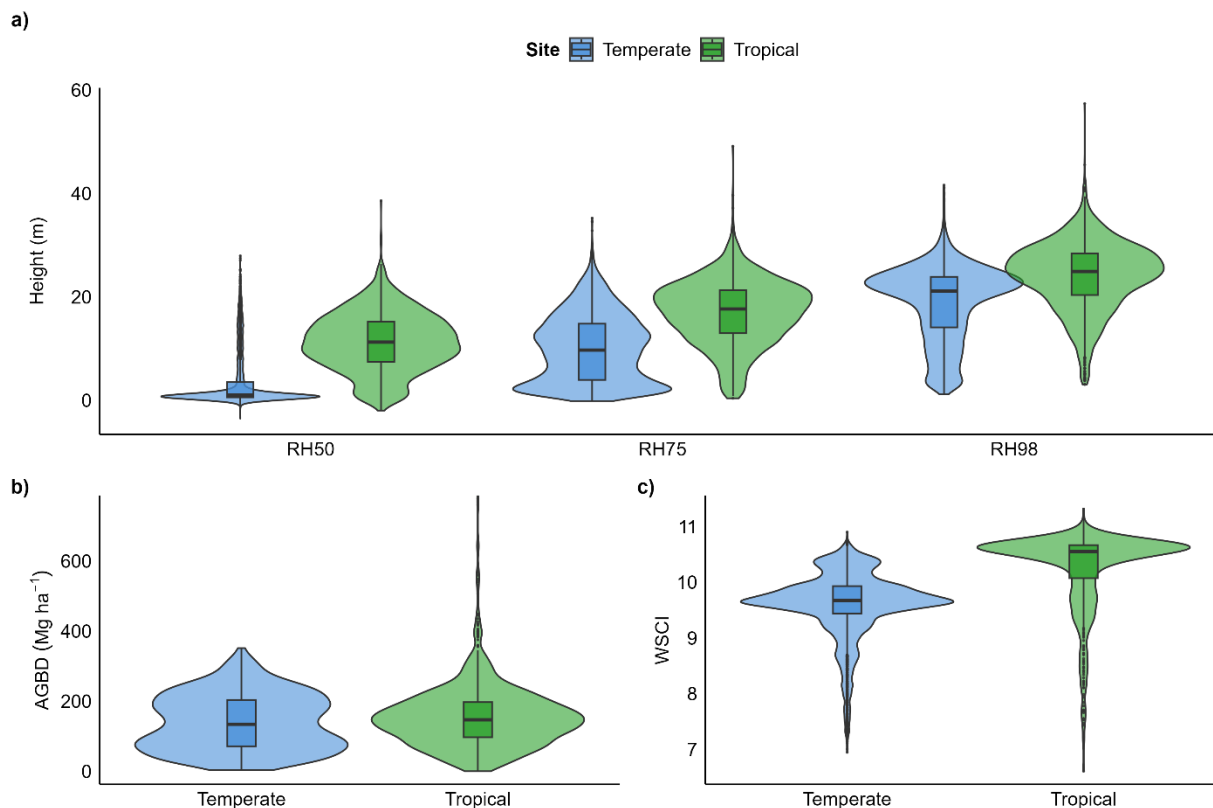
279 Table 4 presents summary statistics for key GEDI-derived variables at each study site. Height percentiles
280 RH50, RH75, and RH98 were selected as representative descriptors of canopy vertical structure; lower
281 percentiles (e.g., RH25) were excluded due to frequent negative values arising from terrain estimation
282 artefacts in waveform processing.

283 The tropical site exhibited consistently taller canopies than the temperate site across all height percentiles
284 (RH98: 24.05 ± 6.55 m vs. 18.86 ± 7.21 m). Height variability was greater at the temperate site (RH98
285 $SD = 7.21$ m) compared to the tropical site ($SD = 6.55$ m). Aboveground biomass density was higher at

286 the tropical site ($157.49 \pm 118.35 \text{ Mg ha}^{-1}$) than at the temperate site ($139.51 \pm 79.89 \text{ Mg ha}^{-1}$), with the
 287 tropical distribution showing a wider range ($0.00\text{--}2,884.04 \text{ Mg ha}^{-1}$) and right-skewed shape. Structural
 288 complexity (WSCI) was also higher at the tropical site (10.24 ± 0.72 vs. 9.60 ± 0.59). The distribution of
 289 height percentiles and biomass values across both sites is shown in Fig. 6.

290 **Table 4.** Summary statistics of GEDI-derived forest structural and biomass variables for forested
 291 footprints at each study site. Values are reported as mean \pm standard deviation, with sample size (n) per
 292 product. L2B metrics at the tropical site (n = 16) should be interpreted with caution. Variables RH50,
 293 RH75, and RH98 were selected as representative height percentiles following standard GEDI analysis
 294 practice.

Variable	Unit	Product	Temperate (n)	Temperate (mean \pm SD)	Tropical (n)	Tropical (mean \pm SD)
RH50	m	L2A	5,939	3.56 ± 5.29	1,712	11.28 ± 5.60
RH75	m	L2A	5,939	9.99 ± 6.48	1,712	16.93 ± 6.24
RH98	m	L2A	5,939	18.86 ± 7.21	1,712	24.05 ± 6.55
cover	—	L2B	3,609	0.31 ± 0.20	16*	0.44 ± 0.27
pai	$\text{m}^2 \text{ m}^{-2}$	L2B	3,609	0.91 ± 1.07	16*	1.47 ± 1.27
fhd normal	—	L2B	3,609	2.85 ± 0.48	16*	2.85 ± 0.31
agbd	Mg ha^{-1}	L4A	430	139.51 ± 79.89	1,493	157.49 ± 118.35
wsci	—	L4C	4,940	9.60 ± 0.59	621	10.24 ± 0.72



296 **Figure 6.** Distribution of GEDI-derived forest structural variables for forested footprints at the temperate (blue) and
 297 tropical (green) study sites. (a) Relative height percentiles (RH50, RH75, RH98) from L2A. (b) Aboveground
 298 biomass density (AGBD) from L4A. (c) Waveform Structural Complexity Index (WSCI) from L4C. Violin plots
 299 show the probability density of each distribution; embedded boxplots indicate the median, interquartile range, and
 300 outliers.

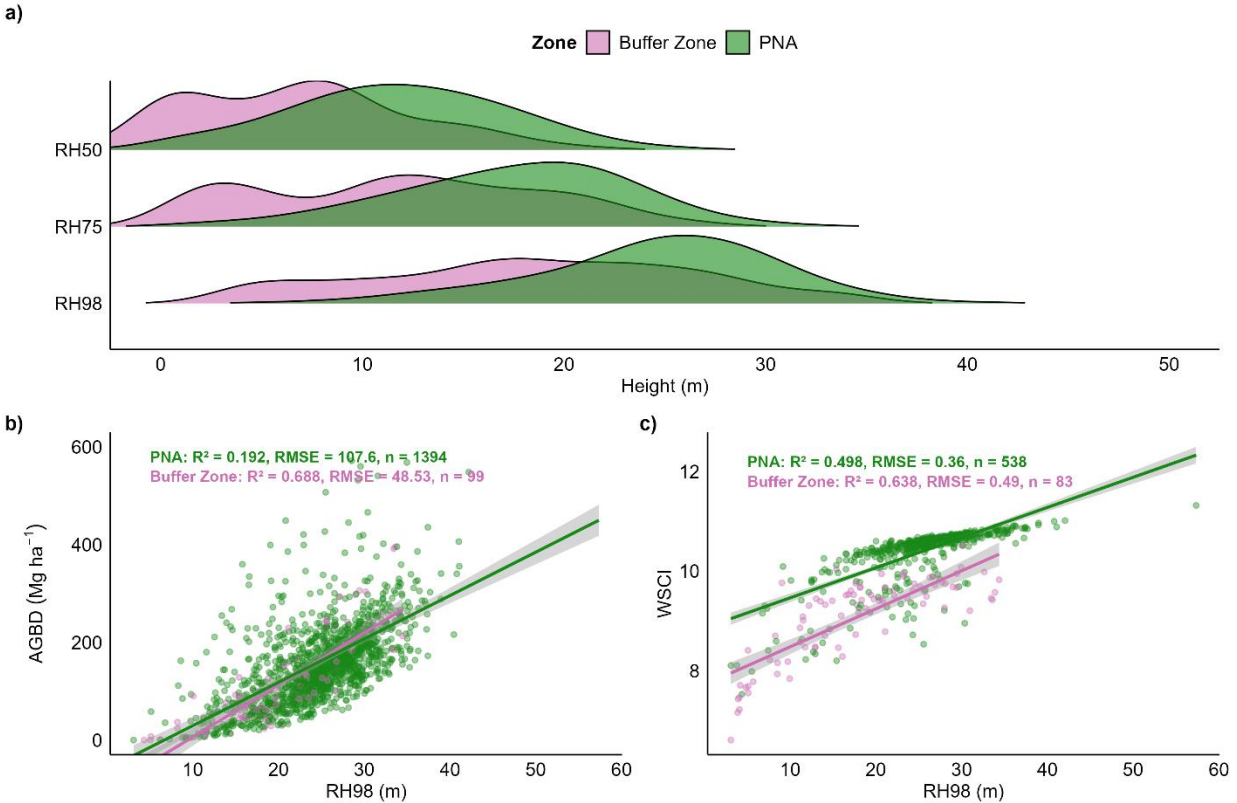
301 **5.2.1. Forest structure inside and outside protected area**

302 Footprints at the tropical site were classified according to their location within the Tambopata National
 303 Reserve (PNA, n = 1,536) or its surrounding buffer zone (BZ, n = 176). Table 5 and Fig. 7 summarise the
 304 results.

305 Forested footprints within the PNA exhibited consistently higher values across all evaluated variables
 306 compared to the buffer zone (Table 5). Canopy height differences were most pronounced at upper
 307 percentiles (RH98: 24.68 ± 6.06 m in PNA vs. 18.48 ± 7.94 m in BZ), while AGBD was 38% higher
 308 inside the reserve (160.41 vs. 116.34 Mg ha⁻¹). WSCI also showed clear separation between zones (10.42
 309 ± 0.51 vs. 9.09 ± 0.82). Linear relationships between RH98 and both AGBD and WSCI were positive in
 310 both zones (Fig. 7b, c), with the buffer zone showing higher R² values (AGBD: R² = 0.69; WSCI: R² =
 311 0.64) compared to the PNA (AGBD: R² = 0.19; WSCI: R² = 0.50), though based on substantially smaller
 312 sample sizes (n = 99 and n = 83, respectively).

313 **Table 5.** GEDI-derived forest structural and biomass variables for forested footprints inside the
 314 Tambopata National Reserve (PNA) and its buffer zone (BZ) at the tropical study site. Values are reported
 315 as mean \pm standard deviation.

Variable	Unit	Product	PNA (n)	PNA (mean \pm SD)	BZ (n)	BZ (mean \pm SD)
RH50	m	L2A	1,536	11.78 ± 5.42	176	6.89 ± 5.26
RH75	m	L2A	1,536	17.51 ± 5.89	176	11.82 ± 6.88
RH98	m	L2A	1,536	24.68 ± 6.06	176	18.48 ± 7.94
agbd	Mg ha ⁻¹	L4A	1,394	160.41 ± 119.73	99	116.34 ± 87.38
wsci	—	L4C	538	10.42 ± 0.51	83	9.09 ± 0.82



316

317 **Figure 7.** GEDI-derived forest structural differences between the Tambopata National Reserve (PNA, green) and its
 318 buffer zone (BZ, purple) at the tropical study site. (a) Density ridgeline plots of relative height percentiles (RH50,
 319 RH75, RH98) from L2A showing the shift toward taller canopies inside the reserve. (b) Relationship between
 320 canopy height (RH98) and aboveground biomass density (AGBD, L4A) with linear regression fits and statistics per
 321 zone. (c) Relationship between canopy height (RH98) and waveform structural complexity index (WSCI, L4C).
 322 Shaded areas indicate 95% confidence intervals.

323 5.2.2. Seasonal variation in canopy structure at the temperate site

324 To assess the capacity of the GEDI dataset to capture phenological dynamics, footprints at the temperate
 325 site were classified into vegetative (April–October, $n = 2,668$) and non-vegetative (November–March, $n =$
 326 $3,271$) periods. Table 6 presents the results for L2A height percentiles and L2B canopy structure metrics.

327 Canopy cover and plant area index showed clear seasonal differences, with higher values during the
 328 vegetative period (cover: 0.37 ± 0.27 vs. 0.27 ± 0.12 ; PAI: 1.32 ± 1.58 vs. 0.68 ± 0.48), consistent with
 329 the presence of deciduous foliage. In contrast, canopy height (RH98) remained stable across seasons
 330 (18.93 ± 7.41 vs. 18.79 ± 7.03 m), confirming that height metrics are largely insensitive to phenological
 331 state. Foliage height diversity (fhd_normal) showed no seasonal variation (2.85 in both periods). The
 332 most pronounced seasonal signal was observed in RH50, which increased from 1.27 ± 1.75 m in the non-
 333 vegetative period to 6.36 ± 6.66 m during the vegetative period, reflecting the increased interception of
 334 laser energy by mid-canopy foliage.

335 **Table 6.** Seasonal comparison of GEDI-derived canopy height and structure variables at the temperate
 336 study site. Vegetative period: April–October; non-vegetative period: November–March. L2B metrics
 337 (cover, PAI, fhd_normal).

Variable	Unit	Product	Vegetative (n)	Vegetative (mean ± SD)	Non- vegetative (n)	Non-vegetative (mean ± SD)
RH50	m	L2A	2,668	6.36 ± 6.66	3,271	1.27 ± 1.75
RH75	m	L2A	2,668	11.44 ± 7.27	3,271	8.81 ± 5.48
RH98	m	L2A	2,668	18.93 ± 7.41	3,271	18.79 ± 7.03
cover	—	L2B	1,308	0.37 ± 0.27	2,301	0.27 ± 0.12
pai	m ² m ⁻²	L2B	1,308	1.32 ± 1.58	2,301	0.68 ± 0.48
fhd_normal	—	L2B	1,308	2.85 ± 0.50	2,301	2.85 ± 0.48

338

339 **6. Discussion**

340 **6.1. Methodological contribution and positioning within existing tools**

341 The principal contribution of GEDIMetrics is an automated process of footprint-level fusion of L2A,
 342 L2B, L4A, and L4C products through the shot_number identifier within a unified GIS environment. This
 343 multi-product integration approach builds on the processing logic originally proposed by (Corado and
 344 Godinho 2025), extending it from a command-line pipeline to an interactive graphical workflow
 345 embedded in QGIS. The tool addresses a long-standing operational bottleneck: users must currently
 346 navigate independently distributed HDF5 files across several GEDI products organised by beam, each
 347 with product-specific quality logic and filtering (Dubayah et al. 2020a; De Conto et al. 2024) and align
 348 footprints across software environments before any analysis can begin. Through its graphical interface,
 349 GEDIMetrics removes this requirement, allowing users to select products, variables, quality thresholds,
 350 and join strategies without scripting, lowering the barrier for non-programming users. Direct export to
 351 GeoPackage and GeoParquet makes outputs usable in GIS and interoperable with Python and R
 352 workflows, supporting reproducible and open-source forest analysis workflows in line with broader
 353 FAIR-oriented (Findability, Accessibility, Interoperability, and Reusability) data management and open-
 354 science practices (Wilkinson et al. 2016; Atkins et al. 2022).

355 GEDIMetrics complements existing tools, each addressing a different segment of the GEDI workflow.
 356 Libraries such as rGEDI (Silva et al. 2020), pyGEDI (Serna and Hernandez-Serna 2020), and GEDI-
 357 Pipeline (Corado and Godinho 2025) enable flexible scripted processing but require coding expertise and
 358 do not natively produce multi-product datasets. NASA's EarthData Search supports discovery and
 359 download but lacks quality filtering, or product integration (NASA 2026). The gediDB Python package
 360 (Besnard et al. 2025) offers scalable TileDB-based querying of pre-ingested L2A–L4C data but lacks an
 361 interactive GIS interface accessible to users with limited coding experience, while geolocation correction
 362 methods such as GeoGEDI (Schleich et al. 2023) and GEDICorrect (Corado et al. 2025) address the
 363 complementary problem of improving GEDI footprint positional accuracy and could be coupled with
 364 GEDIMetrics in extended workflows. Within the QGIS plugin ecosystem, GEDIMetrics is among the first
 365 tools designed for spaceborne LiDAR data processing. Its outputs can be directly combined with optical
 366 remote sensing data acquired through other QGIS plugins (e.g., Semi-Automatic Classification Plugin;
 367 Congedo 2021) or cloud-based platforms such as Google Earth Engine (Gorelick et al. 2017),
 368 positioning GEDIMetrics as a user-friendly, GIS-integrated entry point for multi-source analysis.

369 **6.2. Multi-product integration: implications and applicability**

370 The case study, conducted across two geographically distinct areas (~100 km² each), exposes a
371 fundamental constraint of GEDI-based analysis. Considering that GEDI is mounted on the ISS, footprint
372 distribution is governed by ISS orbital geometry rather than a regular repeat-pass scheme, producing
373 markedly uneven spatial and temporal coverage (Dubayah et al. 2020a): the temperate site in France
374 yielded 96 granules, compared to only 23 granules at the tropical site in Peru over a comparable temporal
375 range. Beyond acquisition volume, the amount of usable information varies substantially depending on
376 applied filters and product-specific quality criteria, as demonstrated by the contrasting retention rates
377 observed between the temperate and tropical sites for L2B canopy structure and L4A biomass. These
378 asymmetries are shaped by the analytical decisions that GEDIMetrics makes explicit through its interface:
379 join strategy, quality thresholds, and beam sensitivity, which can be adjusted according to vegetation
380 density or analysis scale (e.g., (Rajab Pourrahmati et al. 2023; Oliveira et al. 2023)). By exposing these
381 choices through a graphical interface rather than embedding them as fixed defaults, GEDIMetrics makes
382 methodological decisions transparent and reproducible, regardless of the study area or ecosystem under
383 analysis.

384 The plugin's versatility was illustrated through two contrasting examples: comparative analysis of forest
385 structure inside and outside the Tambopata National Reserve in the Peruvian Amazon, a region affected
386 by gold-mining-driven deforestation (Asner et al. 2013; Caballero Espejo et al. 2018), and detection of
387 seasonal variation in canopy structure at the temperate site. Similar workflows can be extended to other
388 forest-monitoring applications where integrated structural and biomass information at the footprint level
389 is required. The applicability of such analyses will depend on study area size, ecosystem characteristics,
390 and GEDI footprint availability, which varies substantially between regions due to ISS orbital coverage
391 and could be complemented with ICESat-2 data in boreal and high-latitude regions (Duncanson et al.
392 2026).

393 **6.3. Limitations and future development**

394 GEDIMetrics depends on authenticated access to NASA EarthData and the stability of the CMR API.
395 Institutional firewall restrictions are partially mitigated by the plugin's support for personal access tokens
396 as an alternative to standard credentials. Processing is currently single-machine and sequential, which can
397 result in long execution times for large ROIs; however, the modular pipeline architecture facilitates future
398 implementation of parallelised downloads and batch processing of multiple non-contiguous areas.
399 Installation requires careful handling of geospatial and HDF5 dependencies (h5py, geopandas, shapely,
400 fiona, rtree), which can conflict with other QGIS Python environments. On Windows systems, the
401 OSGeo4W distribution provides a self-contained environment that resolves these conflicts, and future
402 releases will aim to simplify dependency management across platforms. GEDI footprint geolocation
403 uncertainty (~10 m at 1 σ for v002; (Tang et al. 2023)) is not currently corrected within the plugin, but its
404 modular design allows straightforward integration with external correction tools such as GeoGEDI
405 (Schleich et al. 2023) and GEDICorrect (Corado et al. 2025).

406 The current release targets four GEDI products focused on forest vertical structure (L2A, L2B, L4A,
407 L4C), providing a solid foundation for uncoming extensions. Development priorities include polygon-
408 level summary statistics, retention diagnostics quantifying footprint loss at each filtering stage, and in-
409 plugin visualisation of vertical foliage profiles available through L2B variables (e.g., `pai_z`, `cover_z`,
410 `pavd_z`). Looking further ahead, GEDIMetrics could evolve toward a hybrid local–cloud workflow.
411 NASA EarthData increasingly supports cloud-native data discovery, and STAC-based cataloguing is
412 being adopted across the EarthData datasets. Integration with cloud-hosted archives such as `gediDB`

413 (Besnard et al. 2025) would allow large-scale data retrieval to be delegated to remote infrastructure while
414 GEDIMetrics preserves its role as an accessible, GIS-integrated analysis front-end.

415 **7. Conclusions**

416 GEDIMetrics integrates the full GEDI processing chain: granule discovery, authenticated download,
417 variable extraction, quality filtering, spatial subsetting, and multi-product merging into a single graphical
418 workflow within QGIS, accessible to non-programming users. Its core contribution is the automated
419 footprint-level fusion of L2A, L2B, L4A, and L4C products through the shot_number identifier,
420 producing analysis-ready outputs in GeoPackage and GeoParquet formats interoperable with Python and
421 R workflows. Users interactively select products, variables, quality thresholds, and join strategies,
422 replacing multi-step custom scripting with a transparent and reproducible procedure.

423 The plugin was tested across two contrasting forest ecosystems: temperate mixed forest in northeastern
424 France and humid tropical rainforest in Madre de Dios, Peru, spanning different canopy conditions,
425 footprint availability, and quality-flag retention behaviour. The case study confirmed functionality and
426 effective multi-product data availability. The workflow can be extended to other forest-monitoring
427 applications where integrated structural and biomass information at the footprint level is required.
428 GEDIMetrics is freely distributed through the official QGIS Plugin Repository and on GitHub under the
429 GNU General Public License, with planned extensions toward parallelised processing, cloud-native data
430 access, and broader product support.

431 **Competing Interests:** The authors declare that they have no competing interests.

432

433 **References**

- 434 Asner GP, Lactayo W, Tupayachi R, Luna ER (2013) Elevated rates of gold mining in the Amazon
435 revealed through high-resolution monitoring. *Proc Natl Acad Sci USA* 110:18454–18459.
436 <https://doi.org/10.1073/pnas.1318271110>
- 437 Atkins JW, Stovall AEL, Alberto Silva C (2022) Open-Source tools in R for forestry and forest ecology.
438 *Forest Ecology and Management* 503:119813. <https://doi.org/10.1016/j.foreco.2021.119813>
- 439 Besnard S, Dombrowski F, Holcomb A (2025) gediDB: A toolbox for processing and providing Global
440 Ecosystem Dynamics Investigation (GEDI) L2A-B and L4A-C data. *JOSS* 10:8593.
441 <https://doi.org/10.21105/joss.08593>
- 442 Bourgoin C, Ameztoy I, Verhegghen A, et al (2024) Global map of forest cover 2020 - version 2
- 443 Caballero Espejo J, Messinger M, Román-Dañobeytia F, et al (2018) Deforestation and Forest
444 Degradation Due to Gold Mining in the Peruvian Amazon: A 34-Year Perspective. *Remote*
445 *Sensing* 10:1903. <https://doi.org/10.3390/rs10121903>
- 446 Congedo L (2021) Semi-Automatic Classification Plugin: A Python tool for the download and processing
447 of remote sensing images in QGIS. *JOSS* 6:3172. <https://doi.org/10.21105/joss.03172>
- 448 Coops NC, Tompalski P, Goodbody TRH, et al (2023) Framework for near real-time forest inventory
449 using multi source remote sensing data. *Forestry: An International Journal of Forest Research*
450 96:1–19. <https://doi.org/10.1093/forestry/cpac015>

451 Corado L, Godinho S (2025) GEDI-Pipeline

452 Corado L, Godinho S, Silva CA, et al (2025) GEDICorrect: A Scalable Python Tool for Orbit-, Beam-,
453 and Footprint-Level GEDI Geolocation Correction

454 De Conto T, Armston J, Dubayah R (2024) Characterizing the structural complexity of the Earth's forests
455 with spaceborne lidar. *Nat Commun* 15:8116. <https://doi.org/10.1038/s41467-024-52468-2>

456 Dubayah R, Armston J, Kellner JR, et al (2022) GEDI L4A Footprint Level Aboveground Biomass
457 Density, Version 2.1. ORNL DAAC, Oak Ridge, Tennessee, USA

458 Dubayah R, Blair JB, Goetz S, et al (2020a) The Global Ecosystem Dynamics Investigation: High-
459 resolution laser ranging of the Earth's forests and topography. *Science of Remote Sensing*
460 1:100002. <https://doi.org/10.1016/j.srs.2020.100002>

461 Dubayah R, Hofton M, Blair J, et al (2020b) GEDI L2A elevation and height metrics data global footprint
462 level V001. NASA EOSDIS Land Processes Distributed Active Archive Center (DAAC) data set
463 GEDI02_A. 001

464 Dubayah R, Tang H, Armston J, et al (2021) GEDI L2B Canopy Cover and Vertical Profile Metrics Data
465 Global Footprint Level V002. NASA EOSDIS Land Processes DAAC

466 Duncanson L, Montesano PM, Neuenschwander A, et al (2026) Global and boreal estimates of woody
467 aboveground biomass for 2020: Filling GEDI'S northern data gap with ICESat-2 and harmonized
468 Landsat Sentinel-2. *Remote Sensing of Environment* 340:115406.
469 <https://doi.org/10.1016/j.rse.2026.115406>

470 European Environment Agency (2024) Dominant Leaf Type 2018 - Present (raster 10m), Europe, yearly,
471 Nov. 2024

472 FAO (2025) Global Forest Resources Assessment 2025. FAO, Rome, Italy

473 Goetz S, Dubayah R (2011) Advances in remote sensing technology and implications for measuring and
474 monitoring forest carbon stocks and change. *Carbon Management* 2:231–244.
475 <https://doi.org/10.4155/cmt.11.18>

476 Gorelick N, Hancher M, Dixon M, et al (2017) Google Earth Engine: Planetary-scale geospatial analysis
477 for everyone. *Remote Sens Environ* 202:18–27. <https://doi.org/10.1016/j.rse.2017.06.031>

478 Graser A, Sutton T, Bernasocchi M (2025) The QGIS project: Spatial without compromise. *Patterns*
479 6:101265. <https://doi.org/10.1016/j.patter.2025.101265>

480 Hakkenberg CR, Tang H, Burns P, Goetz SJ (2023) Canopy structure from space using GEDI lidar.
481 *Frontiers in Ecol & Environ* 21:55–56. <https://doi.org/10.1002/fee.2585>

482 Kluyver Thomas, Ragan-Kelley Benjamin, Pérez-Fernando, et al (2016) Jupyter Notebooks
483 – a publishing format for reproducible computational workflows. In: *Positioning and*
484 *Power in Academic Publishing: Players, Agents and Agendas*. IOS Press

485 Markus T, Neumann T, Martino A, et al (2017) The Ice, Cloud, and land Elevation Satellite-2 (ICESat-2):
486 Science requirements, concept, and implementation. *Remote Sensing of Environment* 190:260–
487 273. <https://doi.org/10.1016/j.rse.2016.12.029>

488 Martinoli T, Sona G, Venuti G, et al (2026) A flexible QGIS plugin for mapping burned areas and burn
489 severity from multispectral remote sensing imagery. *European Journal of Remote Sensing*
490 59:2646571. <https://doi.org/10.1080/22797254.2026.2646571>

491 Meng Q, Leau Y-B, Shi J, Zhou J (2026) Multi-Source Remote Sensing Data Fusion for Aboveground
492 Biomass Estimation in Tropical Forests: Recent Advances, Challenges, and Future Trends. *IEEE*
493 Access 14:4688–4732. <https://doi.org/10.1109/ACCESS.2025.3649092>

494 Næsset E, Gobakken T, Solberg S, et al (2011) Model-assisted regional forest biomass estimation using
495 LiDAR and InSAR as auxiliary data: A case study from a boreal forest area. *Remote Sensing of*
496 *Environment* 115:3599–3614. <https://doi.org/10.1016/j.rse.2011.08.021>

497 NASA (2026) Earthdata Search. <https://search.earthdata.nasa.gov/search>. Accessed 3 May 2026

498 Oliveira P, Zhang X, Peterson B, Ometto JP (2023) Using simulated GEDI waveforms to evaluate the
499 effects of beam sensitivity and terrain slope on GEDI L2A relative height metrics over the
500 Brazilian Amazon Forest. *Science of Remote Sensing* 7:100083.
501 <https://doi.org/10.1016/j.srs.2023.100083>

502 Pacsi R, La Torre S, Balbuena H, et al (2026) MAAP #241: Rapid Expansion of Illegal Gold Mining in
503 Tambopata National Reserve (Southern Peruvian Amazon). In: MAAP.
504 <https://www.maaprogram.org/mining-peru-tambopata/>. Accessed 13 May 2026

505 Pardini M, Armston J, Qi W, et al (2019) Early Lessons on Combining Lidar and Multi-baseline SAR
506 Measurements for Forest Structure Characterization. *Surv Geophys* 40:803–837.
507 <https://doi.org/10.1007/s10712-019-09553-9>

508 Potapov P, Li X, Hernandez-Serna A, et al (2021) Mapping global forest canopy height through
509 integration of GEDI and Landsat data. *Remote Sens Environ* 253:112165.
510 <https://doi.org/10.1016/j.rse.2020.112165>

511 Rajab Pourrahmati M, Baghdadi N, Fayad I (2023) Comparison of GEDI LiDAR Data Capability for
512 Forest Canopy Height Estimation over Broadleaf and Needleleaf Forests. *Remote Sensing*
513 15:1522. <https://doi.org/10.3390/rs15061522>

514 Schleich A, Durrieu S, Soma M, Vega C (2023) Improving GEDI Footprint Geolocation Using a High-
515 Resolution Digital Elevation Model. *IEEE J Sel Top Appl Earth Observations Remote Sensing*
516 16:7718–7732. <https://doi.org/10.1109/JSTARS.2023.3298991>

517 Serna E, Hernandez-Serna A (2020) pyGEDI: NASA’s Global Ecosystem Dynamics Investigation (GEDI)
518 mission data extraction, analysis, processing and visualization. version 0.2, April. 5th 2020

519 Silva CA, Hamamura C, Valbuena R, et al (2020) rGEDI: an R package for NASA’s global ecosystem
520 dynamics investigation (GEDI) data visualizing and processing

521 Tang H, Stoker J, Luthcke S, et al (2023) Evaluating and mitigating the impact of systematic geolocation
522 error on canopy height measurement performance of GEDI. *Remote Sensing of Environment*
523 291:113571. <https://doi.org/10.1016/j.rse.2023.113571>

524 Torresani M, Moudry V, Hakkenberg C, et al (2026) The role of GEDI spaceborne lidar in biodiversity
525 analyses: a topical review. *Environ Res Lett*. <https://doi.org/10.1088/1748-9326/ae608a>

526 Vangi E, D'Amico G, Francini S, Chirici G (2023) GEDI4R: an R package for NASA's GEDI level 4 A
527 data downloading, processing and visualization. *Earth Sci Inform* 16:1109–1117.
528 <https://doi.org/10.1007/s12145-022-00915-3>

529 Vogeler JC, Fekety PA, Elliott L, et al (2023) Evaluating GEDI data fusions for continuous
530 characterizations of forest wildlife habitat. *Frontiers in Remote Sensing* 4:.
531 <https://doi.org/10.3389/frsen.2023.1196554>

532 Wilkinson MD, Dumontier M, Aalbersberg IjJ, et al (2016) The FAIR Guiding Principles for scientific
533 data management and stewardship. *Sci Data* 3:160018. <https://doi.org/10.1038/sdata.2016.18>

534

535